Is the environmental exposure gap shrinking? Evidence from an extreme multi-exposure index

Glenn Sheriff, Danae Hernandez-Cortes,
TC Chakraborti, Theresa DeConcini*

January 2026

Abstract

Demographic disparities in exposure to various sources of environmental stress are well documented. While specific stressors are linked to adverse health outcomes, there is uncertainty about how they interact. A first step towards evaluating these joint impacts is to understand the degree to which the same individuals are exposed to extreme simultaneous exposure to each stressor. Here, we adapt the Alkire-Foster multi-dimensional poverty measure to rank exposures to multi-dimensional environmental harm in a way that accounts for the frequency, breadth, and severity of exposure among the extremely exposed. This measure can be used to normatively compare distributions of extreme simultaneous exposure for a given group both across time and in comparison with other groups. We use publicly-available data on air toxics, $PM_{2.5}$, and land surface temperature to identify trends in the multi-exposure index for socio-demographic groups based on race/ethnicity and poverty status for 168 U.S. cities. Controlling for city-characteristics, we find persistent, yet narrowing, multi-exposure gaps on the basis of race/ethnicity between people of color (POC) and non-Hispanic White. Within each group, individuals in households above the poverty line fare better than those below, but above-poverty POC have similar multi-exposure to below-poverty non-Hispanic White.

*Sheriff: Arizona State University. Email: gsheriff@asu.edu, Hernandez-Cortes: Arizona State University and NBER. Email: Danae.Hernandez-Cortes@asu.edu Chakraborty: Pacific Northwest National Laboratory. Email: tirthankar.chakraborty@pnnl.gov, DeConcini: Arizona State University. Email: tdeconci@asu.edu. **Acknowledgements:** This work was partially funded by a grant from the National Science Foundation and NASA. We appreciate the comments from Ann Wolverton, Elise Beshears, Cody Miller, Amila Hadziomerspahic, and participants at the EPA Brownbag Seminar, AERE Summer Conference, Yale Environmental, Natural Resource, and Energy Economics seminar series, and ASU School of Sustainability Seminar.

1 Introduction

People of color (POC) bear a disproportionate exposure to a range of environmental stressors such as fine particulate matter ($PM_{2.5}$) (Pope III et al., 2002; Kaufman et al., 2012; Lefler et al., 2019; Liu et al., 2021; Tessum et al., 2021; Colmer et al., 2020; Sager, 2025), heat (Hsu et al., 2021), and air toxics (Bolin et al., 2000; Morello-Frosch et al., 2001; Wheeler and Ben-Shlomo, 2005; Zwickl et al., 2014). National air quality improvements in recent decades have decreased overall levels of air pollution and narrowed the exposure gap between POC and white communities for air toxics and $PM_{2.5}$ (Ard, 2015; Liu et al., 2021; Currie et al., 2023).[1] At the same time, urban heat poses an increasing health risk for the overall population, and POC in particular, in the U.S. (Hsu et al., 2021; Chakraborty et al., 2023). However, it is unclear what disparities exist in extreme *simultaneous* exposure to these sources of environmental harm and how such exposure may be changing over time. This paper develops a method for estimating disparities in simultaneous exposure to multiple environmental stressors. We apply this method to examine urban areas across the continental U.S., identifying multi-exposure gaps by socio-demographic groups from 2000–2020.

In contrast to the case with single stressors, health impacts arising from simultaneous exposure to multiple environmental stressors are not well understood (Lefler et al., 2019; Escher et al., 2020). An emerging literature suggests that there may be significant interaction effects in the contributions of air pollution and extreme heat to premature mortality (Analitis et al., 2014; Madrigano et al., 2015; Scortichini et al., 2018; Chen et al., 2018; Khomsi et al., 2022; Rahman et al., 2022; Rai et al., 2023). Quantifying simultaneous exposure to different environmental stressors is therefore necessary for understanding the overall benefits of policies that improve environmental quality as well as tracking their distributional implications across demographic groups over time.

Understanding multiple exposure to environmental stressors is relevant for comparing environmental policy options. Implicit in this type of analysis is the ranking of alternative spatial distributions of multiple stressors in a way that allows normative comparisons. These distributions may reflect, for example, modeled pollution attributable to different regulatory policies, exposure levels for various demographic groups, or changes in exposure levels over time for a given group. We show how tools developed in the context of international poverty comparisons may be adapted to facilitate such comparisons in the context of environmental multi-exposure analysis. Such an analytical tool is essential both for understanding the impacts of policy on those most exposed in the population as a whole, as well as better understanding the equity of impacts across demographic groups (Wang et al., 2023).

[1] At a global level, however, income-based air pollution disparities may be increasing (Sager, 2025).

By considering simultaneous exposure, our work extends two main strands of the single-stressor distributional literature. We expand the theoretical literature developing normative methods to rank distributions of environmental outcomes over demographic groups (e.g., Boyce et al., 2016; Sheriff and Maguire, 2020; Venmans and Groom, 2021). We also add to the large empirical literature documenting disparities in environmental outcomes (e.g., Banzhaf et al., 2019; Tessum et al., 2021; Cain et al., 2024), and their evolution over time (Colmer et al., 2020; Hernandez-Cortes and Meng, 2023; Nunez et al., 2024; Colmer et al., 2024; Sager, 2025).

The importance of measuring simultaneous (often referred to as "cumulative") exposure to different environmental stressors has long been recognized (Lee, 2020).[2] Nonetheless, developing methods for quantifying simultaneous exposure to environmental stressors is still an emerging literature. There are two predominant approaches to evaluating disparities in simultaneous impacts: mapping and correlational analysis.

The most common approach taken by both academic researchers and government agencies is to use spatially explicit data to aggregate levels of environmental stress from different sources, perhaps combined with socioeconomic vulnerability indicators, into a single index that can be applied to a given geographical unit (Khanna, 2000; Sadd et al., 2011; Cushing et al., 2015; Faust et al., 2021; Bakkensen et al., 2024). Examples of government mapping tools include the EPA's (now discontinued) EJScreen, and California Office of Environmental Health Hazard Assessment's CalEnviroScreen.[3] This screening approach is useful for policy applications such as issuing permits for polluting facilities, or prioritizing areas for outreach, consultation, and investment in environmental improvements. When issuing permits to polluting facilities, for example, regulators may want to know if the affected areas are already exposed to other pollutants or inhabited by particularly vulnerable populations. There are limitations to this mapping approach, however. Policies that focus on equity goals across geographic units characterized by race or income can actually *reduce* equity across individuals in these demographic groups due to heterogeneity within geographic units. For example, Pollack et al. (2025) find that federal flood-risk reduction policies targeted at sensitive communities defined at the census-tract level performed poorly at improving equity for sensitive households.

The correlation approach evaluates the equity of cumulative exposures by calculating a spatially varying cumulative exposure index (typically a weighted sum of normalized exposures). It then estimates how this index is correlated with variables such as race and income

[2]We use the term simultaneous, rather than cumulative, to draw attention to the fact that our analysis focuses on joint exposures to multiple stressors at a single point in time, rather than cumulative exposure to stressors over time.

[3]For recent reviews of multi-stressor mapping tools, see Besse and Rojas-Rueda (2025) and Joseph (2025).

(see Krieg and Faber, 2004; Pearce et al., 2010; Sicotte, 2010; Boucher et al., 2021; Bakkensen et al., 2024). Studies have also estimated the probability that members of a demographic group are jointly exposed relative to other groups (Jowers et al., 2025). This latter work seeks to understand relative frequency of multiple exposure for different groups. However, it does not describe exposure breadth (the methods are unlikely to be tractable for more than two stressors) or severity (exposure is a binary indicator).

While the map-based and correlation approaches have generated important insights, neither is well suited for making normative comparisons of distributions of multiple stressors. Screening maps are not useful for the ranking of complex alternative multi-exposure distributions in the context of policy analysis. Nor do differences in statistical relationships necessarily reflect differences in desirability—correlations between income and multi-exposure might decrease, for example, even while absolute exposures for low-income individuals increase.

Our work proposes a new method to rank distributions of extreme simultaneous exposure to multiple environmental stressors. In contrast with earlier work that seeks to either map or identify socio-demographic correlations with multiple stressors, our approach is explicitly designed for comparing policy alternatives, estimating differences in exposure inequities across groups, and tracking improvements in exposure across time.

Our approach facilitates explicit normative comparisons, allowing one to evaluate whether a distribution of exposures to a set of environmental stressors is "better" than another. Building on the multidimensional poverty measure developed by Alkire and Foster (2011), the multi-exposure metric accounts for the frequency (number of extremely exposed individuals), breadth (number of dimensions to which these individuals are exposed), and severity (amount above a threshold value) of exposures to extremely-exposed individuals. It allows one to rank distributions of simultaneous exposure across groups and over time in a manner consistent with a set of transparent normative values. Versions of the Alkire and Foster (2011) poverty index are commonly used by organizations such as the UN Development Programme (UNDP, 2025), the World Bank (Lara Ibarra et al., 2025), and the Oxford Poverty and Human Development Initiative (OPHI and UNDP, 2025).

Inevitably, decisions made in the specification of a ranking tool reflect subjective value judgments. In our proposed metric, a key judgment is that society should focus on those most adversely affected (the "environmentally poor") when considering equity of (multidimensional) exposure to environmental harm. Specifically, our focus is on *extremely-exposed* individuals, defined as those who are highly exposed to several stressors. For an individual stressor, "highly" exposed means having an exposure exceeding a given cutoff, and "several" refers to being highly exposed to a minimum threshold of stressors.

We use this approach to calculate extreme multi-exposure for socio-economic groups

varying by race/ethnicity and poverty status across 168 U.S. cities from 2000–2020. Using publicly available data from the Environmental Protection Agency (EPA), the National Aeronautics and Space Administration (NASA), and the Census Bureau, we calculate this measure for distributions of three environmental stressors in urbanized areas of the continental U.S.: $PM_{2.5}$, air toxics, and summer land surface temperature (LST). We use these values to estimate the evolution of national and within-city multi-exposure gaps between demographic groups across the two decades.

Nationally, we find decreases in extreme multi-exposure for each demographic group. Decreases are driven by a shrinking proportion of the population that is extremely exposed. Conditional on being extremely exposed, there were smaller improvements in terms of breadth and severity. Controlling for city-specific effects, we observe narrowing multi-exposure gaps on the basis of race and ethnicity between POC (especially Black populations) and non-Hispanic White populations. Within each group, individuals above poverty fare better than those below, but above-poverty POC have similar multi-exposure to below-poverty non-Hispanic White. Regionally, the intra-city multi-exposure gap appears to be narrowing almost everywhere except Central California and the Gulf Coast of Texas and Louisiana.

The rest of the paper is organized as follows. Section 2 presents the multi-exposure index in detail. Section 3 describes the data used in the analysis. Section 4 calculates the multi-exposure index and uses it to estimate the evolution of demographic disparities over time. Section 5 concludes.

2 The multi-exposure index

To normatively rank spatial distributions of multiple environmental stressors in a manner that satisfies a set of desirable properties, we adapt the multidimensional poverty measure proposed by Alkire and Foster (2011). This measure has several characteristics that make it appealing for ranking simultaneous exposure distributions.

Focus on most exposed: In the context of economic development there is a normative tradition of focusing attention on the welfare of the poor. Poverty reduction is seen as a goal in itself, and the success of anti-poverty policy is measured by its impact on improving the plight of the poor, rather than its impact on the general population. In our context, we begin from the normative position that it is desirable from an environmental policy perspective to alleviate harm to those most exposed to environmental stressors. As such, we use a extreme multi-exposure measure that focuses exclusively on benefits to this group.

Sensitive to exposure "frequency": Given the focus on extremely-exposed individuals, it is desirable that a metric be increasing in the proportion of such individuals in the

population of interest. A key task then is to identify who exactly are the extremely exposed. Similar to Alkire and Foster (2011), we use a two-step identification criterion. The first is to determine a minimum threshold that determines deprivation (i.e., high exposure) in a given dimension (environmental stressor). The second is to determine a cutoff point regarding the minimum number of dimensions in which an individual must be deprived to be considered extremely exposed. A metric satisfies the frequency property if it increases in the proportion of such extremely exposed individuals in a given population. Note that commonly used map-based screening indices do not satisfy this property, nor do statistical correlations between an aggregate index and population characteristics such as race or income.

Sensitive to exposure "breadth": While the frequency property accounts for differences in the number of extremely exposed individuals across exposure scenarios, it does not reflect differences in the number of dimensions in which the exposure threshold is exceeded among the extremely exposed. In contrast, a metric exhibiting the breadth property is increasing in the number of exposure dimensions for which the threshold is exceeded among the extremely exposed as a proportion of the total number of dimensions measured. In other words, a metric sensitive to breadth will improve if, all else equal, the number of dimensions in which an extremely exposed person is deprived decreases.

Sensitive to exposure "severity": While the breadth property accounts for differences in the number of deprived dimensions among the the extremely exposed, it does not account for the degree to which deprivation thresholds are exceeded. A metric satisfying the severity property increases (here, at an increasing rate) in the gap between an extremely exposed individual's exposure level and the threshold in a given dimension.

We use an extreme multi-exposure index adapted from the Alkire and Foster (2011) multi-dimensional poverty index that satisfies the above properties. Formally, let there be D dimensions of environmental stress, indexed $d \in [1, 2, ..., D]$. In our empirical application, environmental stressors are measured for spatial units (census tracts), which we index $u \in [1, ..., U]$, with unit population N_u and total population $N = \sum_{u=1}^{U} N_u$. All individuals residing in a given tract have exposure x_{ud} to stressor d.

Alkire and Foster (2011) focus on "attainments" (e.g., income) for which more is good. In our context, we focus on exposure to environmental harms. While zero is a natural lower bound for good things like income or education, there is no natural upper bound for exposure. We establish a practical upper bound as the 99th percentile of observed exposure (to avoid outliers making the upper bound excessively large). Let $\overline{x}_d$ be the 99^{th} percentile tract exposure in dimension d. We define environmental attainment y_{ud} as the distance between observed exposure and the upper bound: $y_{ud} = \max\{\overline{x}_d - x_{ud}, 0\}$. The D-dimensional vector of attainments for individuals residing in tract u is $\mathbf{y}_u$.

To identify extremely-exposed tracts it is necessary to specify an exposure threshold (analogous to a poverty line) for each environmental stressor. An advantage of the Alkire and Foster (2011) approach is that such determinations are transparently incorporated into the metric in a way that can be easily modified—thus facilitating sensitivity analysis for alternate assumptions. For our empirical application, we define the threshold as the 75^{th} percentile of tract exposure observed in the data.

Let $\mathbf{z} = (z_1, z_2, ..., z_D)$ be the vector of differences between the 99^{th} and 75^{th} percentile exposures. Tracts below an attainment threshold are "deprived" in that environmental characteristic. Function $\theta^0(y_{ud}; z_d)$ indicates those deprived in dimension d:

$$\theta^0(y_{ud}; z_d) = \begin{cases} 1 & y_{ud} \leq z_d, \\ 0 & \text{otherwise.} \end{cases} \tag{1}$$

The next step is to specify the minimum number of dimensions, k, in which a tract must be deprived to be classified as suffering from extreme simultaneous exposure. As with the threshold vector $\mathbf{z}$, the choice of k is subjective, but transparent—and easily changed. Function $\rho(\mathbf{y}_u; k, \mathbf{z})$ indicates extremely exposed tracts:

$$\rho(\mathbf{y}_u; k, \mathbf{z}) = \begin{cases} 1 & \sum_{d=1}^{D} \theta^0(y_{ud}; z_d) \geq k, \\ 0 & \text{otherwise.} \end{cases} \tag{2}$$

Frequency metric F is the proportion of the population suffering from extreme exposure:

$$F = \frac{\sum_{u=1}^{U} N_u \rho(\mathbf{y}_u; k, \mathbf{z})}{N}. \tag{3}$$

Breadth of exposure among the extremely exposed is the total number of deprived dimensions among the extremely exposed divided by the maximum possible number of deprived dimensions among the extremely exposed. This metric, B, is the average share of total dimensions of which the extremely exposed are deprived:

$$B = \frac{\sum_{u=1}^{U} \frac{1}{D} \sum_{d=1}^{D} N_u \rho(\mathbf{y}_u; k, \mathbf{z}) \theta^0(y_{ud}; z_d)}{\sum_{u=1}^{U} N_u \rho(\mathbf{y}_u; k, \mathbf{z})}. \tag{4}$$

We next construct a measure of the severity of deprivations experienced by the extremely exposed. Let $\theta_d^1(\mathbf{y}_u; k, \mathbf{z}) = \frac{z_d - y_{ud}}{z_d} \theta^0(y_{ud}; z_d) \rho(\mathbf{y}_u; k, \mathbf{z})$ denote the normalized attainment shortfall in dimension d of an extremely exposed tract (with value zero for tracts that are not deprived in at least k dimensions). To allow for increasing marginal disutility of depri-

vation let $\theta_d^2(\mathbf{y}_u; k, \mathbf{z}) = \left[\theta_d^1(\mathbf{y}_u; k, \mathbf{z})\right]^2$ denote the square of this normalized shortfall.[4] The normalized severity metric is:[5]

$$S = \frac{\sum_{u=1}^{U} \sum_{d=1}^{D} N_u \theta_d^2(\mathbf{y}_u; k, \mathbf{z})}{\sum_{u=1}^{U} \sum_{d=1}^{D} N_u \rho(\mathbf{y}_u; k, \mathbf{z}) \theta^0(y_{ud}; z_d)}. \tag{5}$$

Its numerator is the sum across extremely exposed individuals of the sum of the squared normalized shortfall in each deprived dimension. The denominator is the sum of all dimensions in which the extremely exposed are deprived. S is thus the average squared normalized shortfall experienced by extremely exposed individuals across all dimensions in which an extremely exposed individual is deprived. Its value is increasing at an increasing rate in the normalized shortfall experienced by an extremely exposed individual.

Combining F, B, and S yields the extreme multi-exposure index, M:

$$M = FBS = \frac{\sum_{u=1}^{U} \frac{1}{D} \sum_{d=1}^{D} N_u \theta_d^2(\mathbf{y}_u; k, \mathbf{z})}{N}. \tag{6}$$

Intuitively, M is the sum of squared normalized shortfalls in all deprived dimensions among the extremely exposed as a proportion of the maximum possible sum of squared normalized shortfalls across all dimensions among the whole population. This metric increases in frequency, breadth, and severity of deprivations among the extremely exposed, justifying its use as a means of ranking the desirability of different joint distributions of environmental harm. It facilitates comparison of distributions of simultaneous exposure at a given level of geographic aggregation (e.g., city), within a given demographic group across time, for example, as well as comparison of distributions across demographic groups in a single period.

For statistical inference, as well as to enable use of multi-exposure in map-based screening tools, we assign the squared normalized attainment shortfall

$$m_u \equiv \frac{1}{D} \sum_{d=1}^{D} \theta_d^2(\mathbf{y}_u; k, \mathbf{z}) \tag{7}$$

from the numerator of Eq. (6) to each tract u.

Empirically, using subscripts g and t to denote demographic group and time period, we

[4]Squaring deprivation also introduces an element of inequality aversion to the severity metric. All else equal, severity cannot be decreased by shifting a unit of exposure from a less-exposed to a more highly-exposed tract.

[5]For simplicity, we have specified equal weight to normalized deprivations in each dimension. Alkire and Foster (2011) show how one can use a general d-dimensional weighting vector $\mathbf{w}$ consisting of positive numbers summing to D to ascribe different importance to each stressor. In Eqs. (2) and (4), $\theta^0(y_{ud}; z_d)$ is replaced with $w_d \theta^0(y_{ud}; z_d)$, and $\theta_d^2(\mathbf{y}_u; k, \mathbf{z})$ is replaced with $w_d \theta_d^2(\mathbf{y}_u; k, \mathbf{z})$ in Eqs. (5) and (6).

use these values to estimate regressions of the type

$$m_{ugt} = \sum_{\tau=1}^{T} \beta_\tau^m \times 1(g = g^1) \times 1(\tau = t) + \phi_{ct} + \epsilon_{ugt} \tag{8}$$

Here, $1(g = g^1)$, is an indicator variable taking a value of 1 for the demographic group of interest, g^1 (e.g., below-poverty Hispanic), to be compared to a reference group g^0 (e.g., above-poverty Hispanic). It is interacted with another indicator variable taking a value of one if τ equals period t. Each tract appears twice in the regression data set, once for each of the two groups. Tract observations are weighted by the population count of the respective demographic group in the tract. This weighting, combined with city-by-time fixed effects ϕ_{ct}, gives the parameter β_t the interpretation of the time-specific within-city multi-exposure gap between groups. Variable ϵ_{ugt} denotes an idiosyncratic error term.

A similar exercise replaces m_{ugt} with analogous values for: frequency,

$$f_u \equiv \ \rho(\mathbf{y}_u; k, \mathbf{z}) \tag{9}$$

$$f_{ugt} = \sum_{\tau=1}^{T} \beta_\tau^f \times 1(g = g^1) \times 1(\tau = t) + \phi_{ct} + \epsilon_{ugt}, \tag{10}$$

$$\tag{11}$$

breadth,

$$b_u \equiv \ \sum_{d=1}^{D} \rho(\mathbf{y}_u; k, \mathbf{z}) \theta^0(y_{ud}; z_d)/D \tag{12}$$

$$b_{ugt} = \sum_{\tau=1}^{T} \beta_\tau^b \times 1(g = g^1) \times 1(\tau = t) + \phi_{ct} + \epsilon_{ugt}, \tag{13}$$

$$\text{for } \rho(\mathbf{y}_u; k, \mathbf{z}) = 1;$$

and severity

$$s_{ud} \equiv \theta_d^2(\mathbf{y}_u; k, \mathbf{z}) \tag{14}$$

$$s_{ugdt} = \sum_{\tau=1}^{T} \beta_\tau^s \times 1(g = g^1) \times 1(\tau = t) + \phi_{ct} + \epsilon_{ugdt}, \tag{15}$$

$$\text{for } \theta^0(y_{ud}; z_d) > 0 \text{ and } \rho(\mathbf{y}_u; k, \mathbf{z}) = 1.$$

These regressions (with census tract observations weighted by relevant population counts)

allow one to track the evolution of per capita gaps in these characteristics as well. The frequency regression tracks differences in the proportion of individuals in each group that are extremely exposed. The breadth regression tracks differences in the number of deprivations among the extremely exposed in each group. The severity metric tracks the average severity per stressor among the extremely exposed. The severity regression is structured slightly differently from the others. Rather than having two observations for each extremely exposed tract (one for each demographic group), there are observations for each demographic group by deprived stressor combination. That is, for $k = 2$ there are either 4 or 6 observations per extremely exposed tract (since there must be at least two deprivations for a tract to be considered extremely exposed). Both the breadth and severity regressions include only tracts that are extremely exposed, i.e., $\rho(\mathbf{y}_u; k, \mathbf{z}) = 1$.

3 Data

We evaluate extreme exposure distributions across 168 U.S. cities from 2000–2020 using publicly available data from the Environmental Protection Agency (EPA), the National Aeronautics and Space Administration (NASA), and the Census Bureau.[6] Specifically, we calculate the extreme multi-exposure index for $PM_{2.5}$, air toxics, and summer LST, using 2010 demographic information from the American Community Survey (ACS). We divide the two decades into three 5-year periods centered on 2000, 2010, and 2020, subject to the exceptions described below.

Air toxics

Air toxics exposure comes from the EPA's Risk-Screening Environmental Indicators Geographic Microdata (RSEI-GM) version 2.3.8 (US EPA, 2019). RSEI-GM has three main components: reported facility releases, modeled chemical dispersion, and chemical toxicity weights. Facility data on stack releases of air toxics are reported in the Toxics Release Inventory (TRI). To avoid spurious changes in measured exposure due to changes of the TRI chemical reporting list over time, we focus attention on the original set of "core" chemicals listed in 1988.[7] Given the facility releases reported in the TRI, RSEI-GM uses the American Meteorological Society/EPA Regulatory Model (AERMOD) to approximate average chemical concentrations in a census tract as a function of facility-specific parameters (such as stack height), meteorology, and chemical-specific decay rates.

[6] We initially focused on the 175 census-defined urbanized areas containing over 250,000 residents. Of these, we dropped the 7 areas with data missing for more than 20 percent of their tracts.

[7] See www.epa.gov/toxics-release-inventory-tri-program/tri-listed-chemicals.

RSEI-GM calculates an aggregate exposure risk by converting the mass of reported releases into "toxicity-weighted" concentrations. Toxicity weights are based on expert elicitation regarding the risk posed by inhalation and reflect the minimum dosage required to affect human health, among other factors. Similar to other studies, we use toxicity-weighted concentrations in a census tract as the measure of local exposure to air toxics (see, for example, Gamper-Rabindran, 2006; Banzhaf and Walsh, 2008; Ard, 2015). Data are available for 2010 tract boundaries until 2020, therefore we use 2017–2020 data to calculate averages for the last period.

There are several limitations of RSEI-GM. Since the underlying TRI data are self reported by facilities, there are potential reporting errors. These may occur due to clerical mistakes, rounding, or deliberate misrepresentation. The EPA engages in several quality assurance practices to reduce chances of misreporting (e.g., following up with facilities that do not submit a current report, but have reported in the past). Statutory provisions on facilities that are required to report (e.g., minimum number of employees) imply that significant sources of releases may not appear in the data. The fact that data are reported annually and dispersal modeling uses annual average wind direction may be problematic if releases occur only during specific times of the year and there are seasonal shifts in weather patterns.

$\mathbf{PM}_{2.5}$

Annual average $PM_{2.5}$ concentrations, measured in $\mu g/m^3$, come from the Privacy-Protected Gridded Environmental Impacts Frame (Voorheis et al., 2024b), which in turn relies on satellite-derived $PM_{2.5}$ concentrations from van Donkelaar et al. (2021) and Shen et al. (2024). Data cover 1998–2022 with a geographic resolution of $0.01^\circ \times 0.01^\circ$. We overlay gridded $PM_{2.5}$ data with 2010 census tract boundaries to calculate area-weighted tract concentrations. One limitation of these data is that annual averages do not capture within-day variation of air pollution or seasonal air quality patterns.

Heat

Human heat stress is affected by several factors including local ambient air temperature, exposure to sunlight, humidity, and wind speed. Unfortunately, it is not tractable to obtain data on all these variables to calculate exposure to heat stress in a consistent manner across space and time since it would require a dense network of ground-based sensors. Instead, we use summer daytime land surface temperature (LST) as a proxy for heat stress. LST has the advantage that it can be readily compiled in a uniform way by combining thermal remote sensing imagery with census tract boundaries in U.S. urbanized areas going back to

the mid-1980s using the Landsat satellite series (Wulder et al., 2022). To estimate LST, we use the Landsat collection 2 LST product, available at roughly 100m resolution every 16 days (Crawford et al., 2023). We average the data covering June, July, and August, representing northern hemisphere summer, after pixel-level cloud and cloud shadow screening using the dataset's uncertainty flags. We use 5-year averages for 2000 and 2020. Since Landsat 5 ended in 2011 and Landsat 7 includes scan line errors that lead to additional uncertainties (Scaramuzza and Barsi, 2005), we only use 2008–2011 data to calculate 2010 averages.

These data have several limitations. First, LST can be a poor quantitative proxy for heat stress (Chakraborty et al., 2022). However, recent modeling exercise for U.S. cities suggest that the direction of heat disparities is similar using LST and measures of heat stress calculated on the basis of air temperature and humidity, but that the magnitudes of the LST differences are higher (Chakraborty et al., 2023). In addition, LST is only observable by satellite under cloudless weather conditions. Using LST as a proxy for heat exposure implicitly assumes these clear sky temperatures are representative of exposures under cloudy conditions. Moreover, because the Landsat overpass is fixed at around 10:30 am local time, these estimates of LST represent a snapshot instead of the full diurnal temperature range. Finally, the 16-day frequency of Landsat leads to a relative under-sampling of the climatology, though this effect is reduced by using data covering up to 15 months (4 to 5 years with 3 months each) for each period of our study.

Demographics

Tract-level demographic information comes from the 5-year U.S. Census American Community Survey (ACS) centered on 2010. It was downloaded from the Census API site using the `getcensus` Stata user-defined program (Zippel et al., 2023). We use tract population counts for non-Hispanic White, and calculate POC as the difference between this value and total tract population. We also use ACS population counts by race and ethnicity by household poverty status for the following groups: Black, Hispanic, American Indian and Alaska Native or Native American[8], non-Hispanic White. Publicly available census data report White by both Hispanic ethnicity and poverty status. Black and Native American by poverty status, however, include both Hispanic and non-Hispanic individuals. Therefore, there is some potential overlap between individuals included in these two groups with those reported in Hispanic. Since we use 2010 demographic values, our analysis abstracts from possible changing population composition due to changes in relative exposure to environmental stressors.[9]

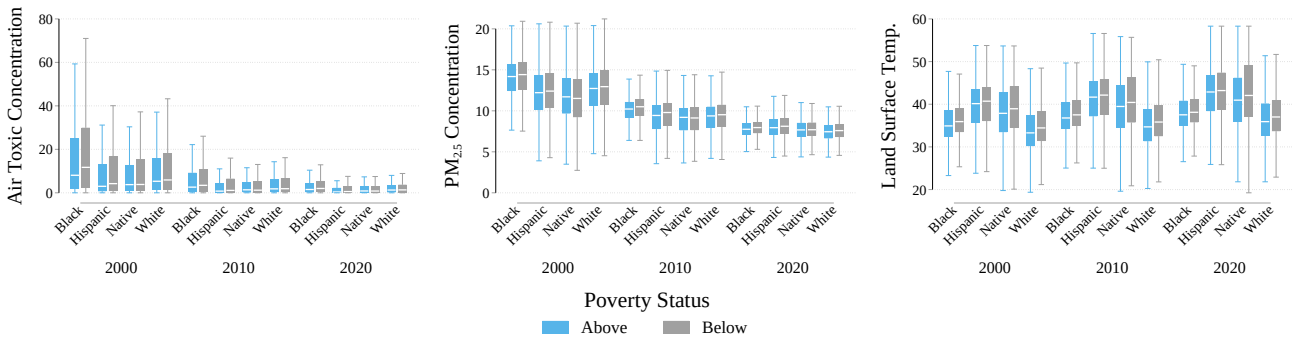
[8]We use the term Native American to refer to American Indian and Alaska Native throughout the rest of the paper.

[9]There is mixed evidence in the literature regarding the importance of such residential sorting on exposure over time. Borsky et al. (2024) found that policies in New York City intended to reduce the urban heat

4 Results

Figure 1 depicts national exposure to the three stressors by demographic group. The population is broken down by race/ethnicity into Black, Native American, Hispanic, and non-Hispanic White. Each demographic group is further broken down by poverty status. Overall, median exposure to air toxics and $PM_{2.5}$ has fallen for all demographic groups. However, for LST exposure has generally increased over time for all groups, likely due to climate change. For all racial/ethnic groups, mean exposure to all stressors for individuals below poverty is higher than their above-poverty counterparts. In general, exposure gaps across groups tend to be more pronounced than income-based gaps within groups. This figure depicts average exposure for the different groups without considering whether the same individuals are simultaneously exposed to multiple stressors.

Figure 1: National exposure levels by stressor, race, and poverty status, 2000–2020



Notes: Air toxic exposure measured in toxicity weighted pounds. $PM_{2.5}$ exposure measured in $\mu g/m^3$. Summer daytime LST exposure measured in °C.

Table 1 presents 2000 and 2020 national values for the extreme multi-exposure index defined in Eq. (6) as well as the frequency, breadth, and severity metrics from Eqs. (3)–(5). Deprivation in a tract-year for a single stressor is being exposed to the top quartile of all tract-year exposure levels across the 168 cities.[10] Severity of tract-year deprivation for a given stressor is the squared normalized difference between the exposure level and the

island effect in poor communities may ultimately have had adverse welfare effects for these groups after sorting took place. In contrast, Currie et al. (2023) and Basu et al. (2025) find little evidence of sorting in response to changes in $PM_{2.5}$.

[10]These thresholds are 8.4 toxicity-weighted concentration for air toxics, 11.8 $\mu g/m^3$ for $PM_{2.5}$, and 40.7 °C for LST. By comparison, the 2024 National Ambient Air Quality Standard for $PM_{2.5}$ is 9 (revised down from 12) $\mu g/m^3$. There are no comparable health-based standards for air toxics or LST.

Table 1: National-level extreme exposure statistics

	Multi-exposure		Frequency		Breadth		Severity	
	2000	2020	2000	2020	2000	2020	2000	2020
Total	0.049	0.006	0.391	0.055	0.696	0.668	0.179	0.153
	(0.009)	(0.002)	(0.046)	(0.025)	(0.014)	(0.001)	(0.025)	(0.024)
Below poverty								
Black	0.096	0.005	0.589	0.063	0.692	0.667	0.236	0.122
	(0.017)	(0.003)	(0.056)	(0.031)	(0.013)	(0.000)	(0.033)	(0.018)
Hispanic	0.070	0.019	0.474	0.142	0.742	0.668	0.200	0.198
	(0.016)	(0.007)	(0.064)	(0.060)	(0.028)	(0.001)	(0.031)	(0.034)
Native American	0.046	0.009	0.331	0.081	0.712	0.667	0.195	0.174
	(0.011)	(0.004)	(0.052)	(0.026)	(0.016)	(.)	(0.029)	(0.041)
non-Hispanic White	0.050	0.004	0.385	0.041	0.684	0.667	0.191	0.146
	(0.008)	(0.001)	(0.039)	(0.012)	(0.007)	(0.000)	(0.019)	(0.026)
Above poverty								
Black	0.078	0.004	0.518	0.054	0.693	0.667	0.219	0.113
	(0.020)	(0.002)	(0.067)	(0.035)	(0.015)	(0.000)	(0.042)	(0.013)
Hispanic	0.057	0.015	0.409	0.124	0.743	0.669	0.187	0.186
	(0.016)	(0.006)	(0.069)	(0.055)	(0.028)	(0.002)	(0.033)	(0.030)
Native American	0.038	0.009	0.311	0.074	0.710	0.668	0.173	0.174
	(0.009)	(0.003)	(0.045)	(0.024)	(0.017)	(0.001)	(0.028)	(0.029)
non-Hispanic White	0.037	0.003	0.348	0.034	0.682	0.668	0.157	0.131
	(0.007)	(0.001)	(0.043)	(0.014)	(0.008)	(0.001)	(0.021)	(0.022)

Notes: Multi-exposure is sum of squared normalized exposure of extremely exposed as proportion of maximum possible squared exposure for given demographic group. Frequency is proportion of extremely exposed in group. Breadth is average fraction of stressors to which extremely exposed have high exposure. Severity is average sum of squared normalized exposure across those stressors for which extremely exposed are deprived. Standard errors clustered by city.

deprivation threshold.[11] The extremely exposed are those who reside in a tract-year that is deprived for two or more stressors. Multi-exposure index values for 2000 are consistent with the prevailing environmental justice literature that finds higher exposure to environmental stressors by race/ethnicity and poverty status. For each demographic group, those living in households below the poverty line have higher multi-exposure scores than those living above the poverty line. Within each poverty classification, values for non-Hispanic White are lower than those for almost all other racial/ethnic groups, except Native American populations. There is further evidence suggesting that race, rather than poverty status, is an important factor in these differences: apart from Native American (and non-Hispanic White), the above poverty category for each racial/ethnic group does not have better (i.e., lower) scores than below-poverty non-Hispanic White.

Overall, there was a substantial drop in index values from 2000 to 2020 (from 0.049 to 0.006), which reflects national improvements in air quality depicted in Figure 1. This improvement was experienced by all racial/ethnic and poverty groups. Relative rankings across groups remained stable, but the absolute value of the gaps significantly narrowed. In 2000 the largest gap was between below-poverty Black (0.096) and above-poverty non-Hispanic White (0.037), while the largest gap in 2020 was between below-poverty Hispanic (0.019) and above-poverty non-Hispanic White (0.003).

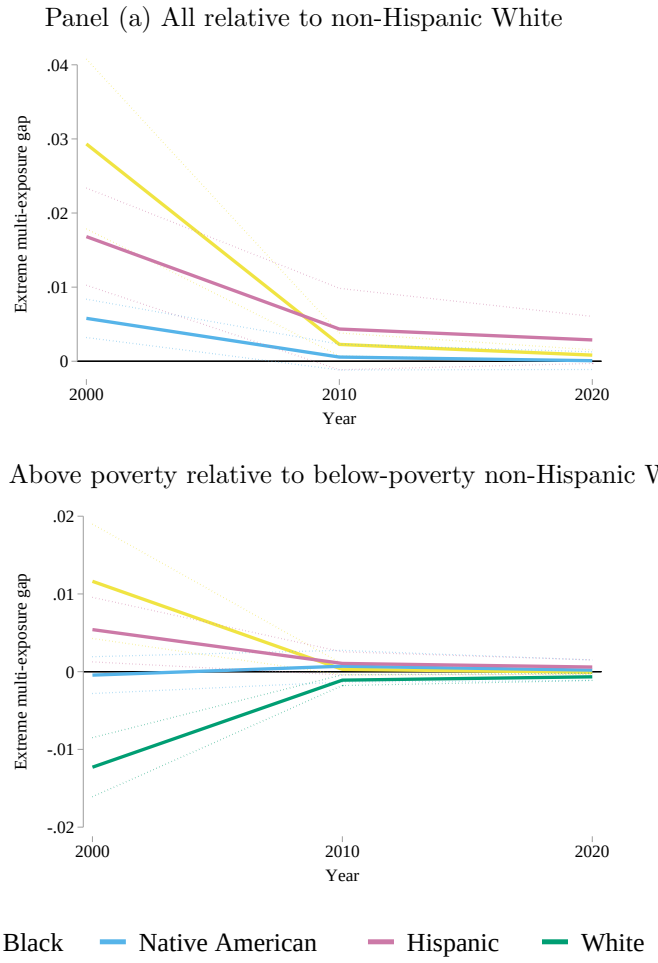
The remaining columns shed light on the factors driving these trends. The overall pattern was driven by a large drop in the proportion of the extremely exposed in the general population from 39.1 to 5.5 percent. This decline took place for all groups with the largest drop (52.6 percent) for below-poverty Black and the smallest for above-poverty Native American (23.7 percent). Regarding breadth, almost all the extremely exposed in each demographic group in 2020 were deprived for only two of the three stressors. This drop is a slight change from 2000 when the proportion of deprived stressors across all extremely-exposed individuals was 0.696. Improvements in exposure severity were also modest for all groups except for Black populations, both above and below the poverty line.

National trends depicted in Figure 1 and Table 1 are partially explained by regional differences in demographic composition. High median Hispanic and Native American exposure to heat, for example, may be driven by a relatively high proportion of these demographic groups living in the Southwest. Intra-city disparities may be more relevant from a policy perspective since they may suggest actions such as permitting, zoning, or anti-discrimination enforcement that are under local jurisdictional control (York et al., 2014; Wang et al., 2023).

Figure 2 illustrates within-city multi-exposure gaps across demographic groups. Each line

[11] The normalized difference is $\max\left\{0, \frac{y_{sd}-z_d}{z_d}\right\}$.

Figure 2: Within-city gaps in extreme multi-exposure, 2000–2020



Notes: Panel (a) shows intra-city gaps in the multi-exposure index for Black, Native American, and Hispanic demographic groups relative to non-Hispanic White. Panel (b) shows gaps for above-poverty Black, Native American, Hispanic, and non-Hispanic White groups relative to below-poverty non-Hispanic White. Lines correspond to parameters β_t^m from Eq. (8). Regressions are weighted by tract population for the relevant demographic groups. Standard errors clustered by city.

in the figure depicts the β_t^m parameter values from Eq. (8) for the indicated racial/ethnic group of interest relative to the reference group. The parameter measures the average within-city difference in the extreme multi-exposure index, M. In Panel (a), the groups of interest are non-Hispanic Black, non-Hispanic Native American, and Hispanic, with the reference group being non-Hispanic White. For Panel (b) the groups of interest are above-poverty Black, Native American, Hispanic, and White and the reference group is below-poverty White.[12] Overall, Panel (a) shows that in 2000 Black, Hispanic, and Native American

[12]Due to data limitations, the Black and Native American racial groups in Panel (b) include those with Hispanic ethnicity.

groups had higher extreme multi-exposure indexes relative to non-Hispanic White. These gaps are statistically significant ($p < 0.05$) for all groups except Native American. The gaps declined over time, and by 2020 were no longer statistically significant.

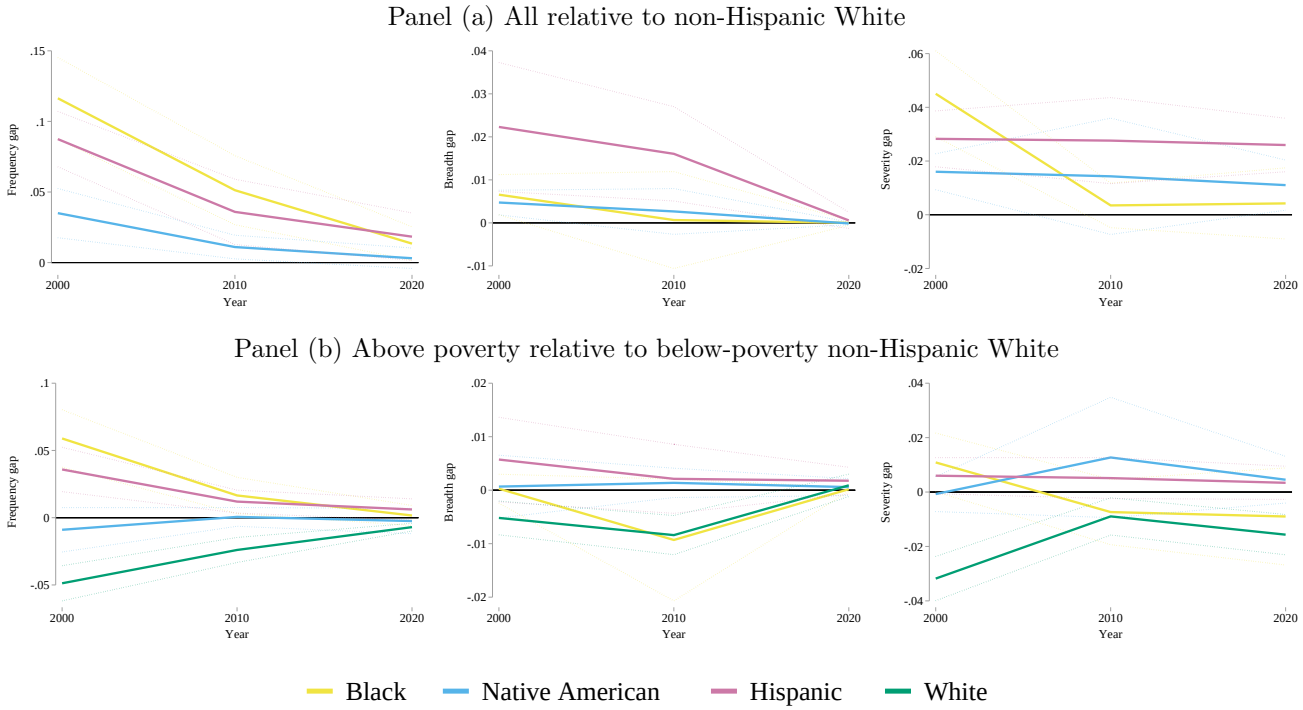
To the extent that environmental amenities are capitalized into real estate values, one might hypothesize that disparities observed in 2 Panel (a) may be due to differences in average income across demographic groups (e.g., the fact that non-Hispanic White tend to have relatively high incomes allows them to effectively outbid other demographic groups in more environmentally desirable neighborhoods). If this narrative were true, however, one might expect above poverty individuals of every demographic group to have better environmental exposure profiles than below-poverty non-Hispanic Whites.

Figure 2 Panel (b) explores the role of income in these disparities. Lines represent gaps between above-poverty members of each racial/ethnic group relative to the below-poverty non-Hispanic White reference group. In 2000, above poverty non-Hispanic White has significantly less extreme multi-exposure than below-poverty non-Hispanic White. Despite their higher income, none of the other above-poverty groups had significantly lower exposure than below-poverty non-Hispanic Whites in 2000. These results are consistent with others in the environmental justice literature (e.g., Tessum et al., 2021; Bakkensen et al., 2024) suggesting that race is a more influential factor than income in driving exposure disparities. By 2020, the gaps between above poverty members of each demographic group and below-poverty non-Hispanic White effectively disappear.

Gaps illustrated in Figure 2 account for frequency, breadth, and severity of extreme exposure. Figure 3 breaks down the extreme multi-exposure index into these three components, showing parameters $\beta_t^f, \beta_t^b, \beta_t^s$ from Eqs. (10), (13), and (15). Leftmost graphs in each panel display only frequency gaps between the proportion of the group of interest that is extremely exposed, relative to the reference group. Middle graphs display only the breadth gap in the average number dimensions in which an extremely exposed tract is deprived as a proportion of the total number of dimensions (in this case, 3). Note that while the frequency regression includes observations for all tracts, the breadth regression only includes extremely exposed tracts. Thus, only the frequency gap (leftmost) will necessarily increase if a tract that disproportionately has residents of the group of interest relative to the reference group becomes extremely exposed. Rightmost graphs display only severity—the average severity of exposure for those dimensions in which an extremely exposed tract is deprived. That is, while the gap in the breadth graph (middle) will necessarily increase if an extremely exposed tract that has a disproportionate number of residents of the group of interest becomes deprived in an additional dimension, the extreme multi-exposure gap will not.

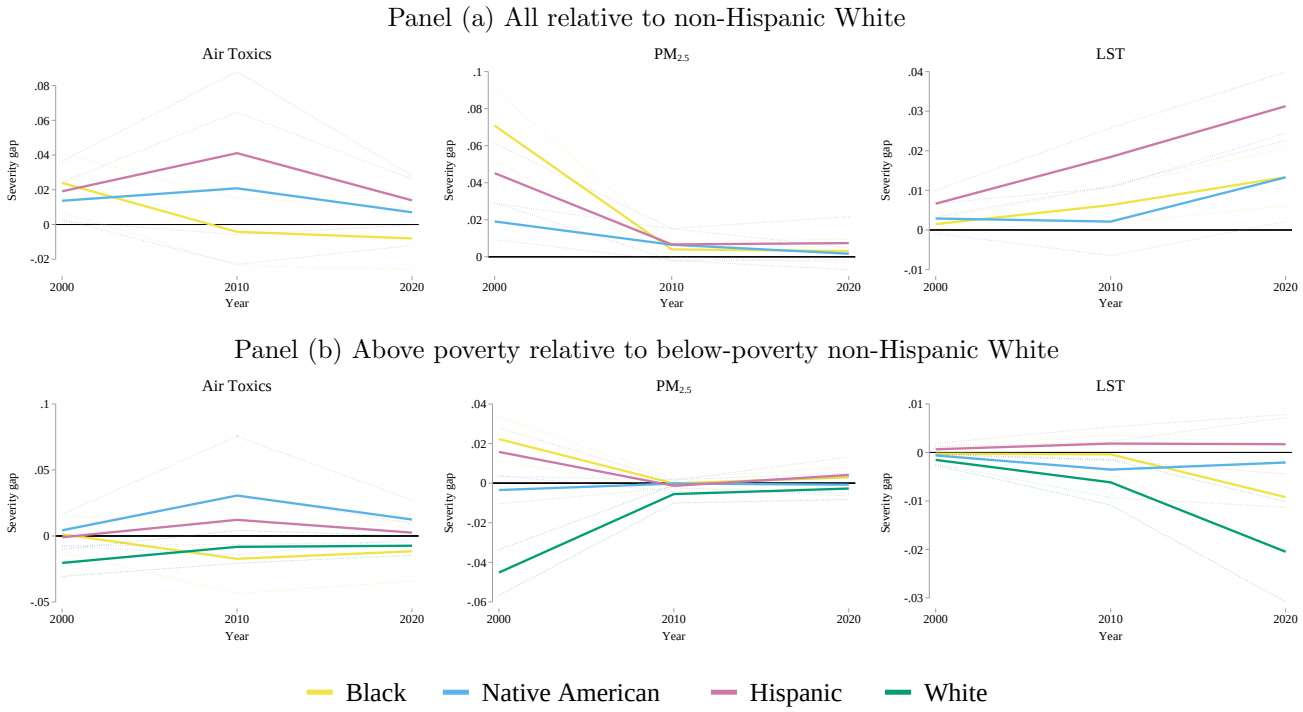
Figure 3 shows a general convergence by race and income over time in the frequency

Figure 3: Within-city gaps in Frequency, Breadth, and Severity, 2000–2020



Notes: Columns of figures depict parameters β_t^f, β_t^b, and β_t^s from Eqs. (10), (13), and (15), respectively. Panel (a) shows intra-city gaps for Black, Native American, and Hispanic demographic groups relative to non-Hispanic White. Panel (b) shows gaps for above-poverty Black, Native American, Hispanic, and non-Hispanic White groups relative to below-poverty non-Hispanic White. Regressions are weighted by tract population for the relevant demographic groups. Standard errors clustered by city.

Figure 4: Trends in within-city severity gaps for each stressor among the extremely exposed



Notes: Panel a) shows single stressor time-varying within-city severity disparities for Black, Native American, and Hispanic relative to non-Hispanic White for 2000–2020. Severity is defined as the squared normalized difference between the exposure and the deprivation threshold defined in Section 2. Panel b) shows time-varying within-city disparities for Black, Native American, Hispanic, and non-Hispanic White groups relative to below poverty non-Hispanic White for 2000–2020. Regressions are weighted by tract population for the relevant demographic groups. Standard errors clustered by city.

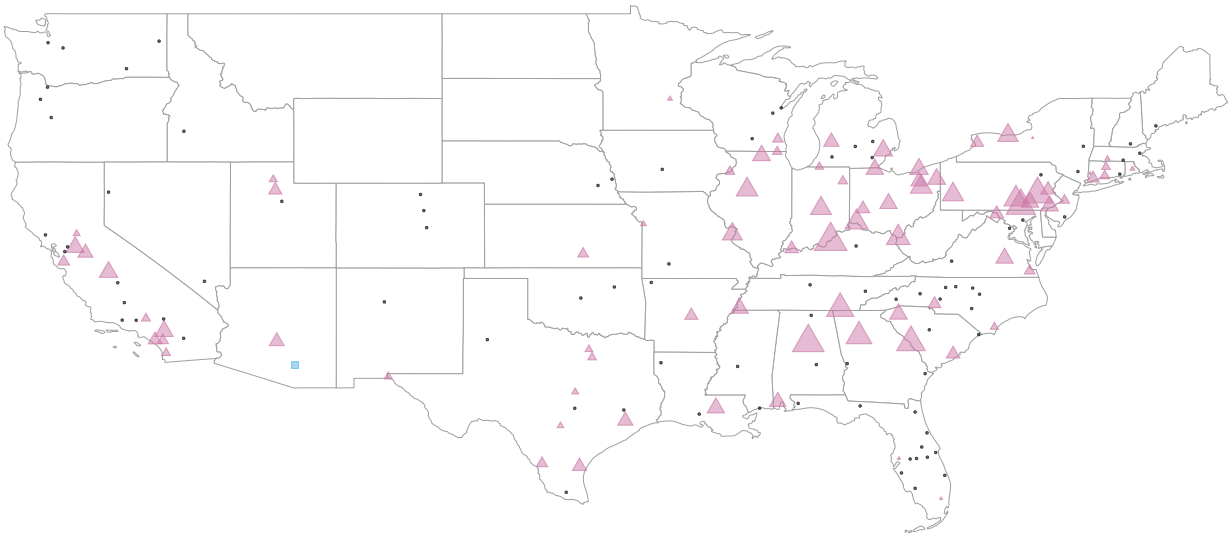
and breadth of extreme exposure. Although the intra-city severity gap between Black and non-Hispanic White has fallen over the two decades, this gap between non-Hispanic White and Hispanic and Native American has remained stable. With respect to poverty status, extremely exposed above-poverty non-Hispanic White has significantly lower severity than extremely exposed below-poverty non-Hispanic Whites. It also remained lower than most of the other above-poverty groups. The exception is Black populations, which went from significantly higher exposure in 2000 to a statistically insignificant gap in 2020.

To explore why severity gaps are not converging, Figure 4 shows these gaps separately for each stressor. Reductions in severity gaps in air toxics and $PM_{2.5}$ have been countered by widening gaps in LST. For Black individuals, the net effect has been a narrowing of the overall severity gap, whereas for Hispanic and Native American, changes in LST exposure have been sufficient to partially offset improvements in the other two stressors.

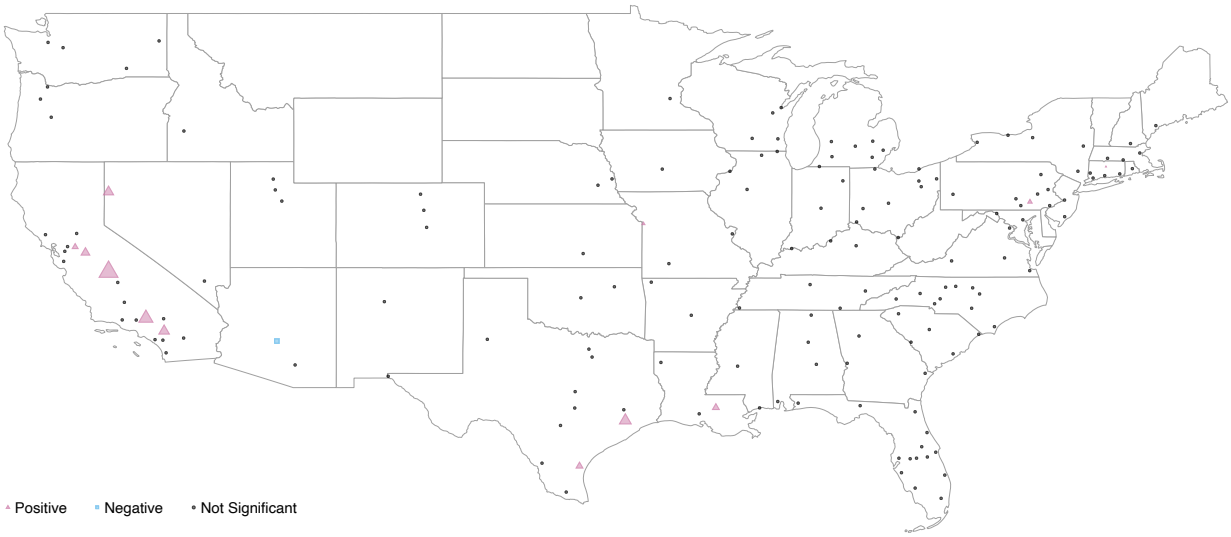
Whereas Figures 2–4 depict average within-city trends, Figure 5 shows how extreme

Figure 5: Differences across time in city-level demographic gaps in multiexposure index

Panel (a) POC – non-Hispanic White, 2000



Panel (b) POC – non-Hispanic White, 2020



Notes: Significant ($p < 0.05$) within-city differences in extreme multi-exposure index between POC and non-Hispanic White. Significant ($p < 0.05$) positive values are depicted with triangles, significant negative values are depicted with squares, and statistically insignificant values are depicted with circles. Size of marker proportional to absolute value of significant difference. Standard errors clustered by census tract.

multi-exposure gaps have changed over time for each city. Markers on each map are proportional to the absolute value of parameter β_t^m estimated in Eq. (8) separately for each city-year, with the group of interest being POC (i.e., everyone who does not identify as non-Hispanic White). Significant (p <0.05) positive values are depicted with triangles, significant negative values are depicted with squares, and statistically insignificant values are depicted with circles. The size of the marker is proportional to the magnitude of the values. In 2000 extreme multi-exposure gaps were widespread in cities throughout the continental U.S. Among statistically significant gaps, the vast majority of cases (77) show POC having higher extreme multi-exposure than non-Hispanic White (only 1 had the reverse). By 2020, almost all but 10 significant gaps had been eliminated. Exceptions are primarily in California's Central Valley and along Texas and Louisiana Gulf Coast.

Sensitivity Analysis

Calculation of the multi-exposure index depends on various parameters, including: the threshold level to determine the severity of exposure and the minimum number of deprivations to qualify as extremely exposed. In this section, we explore sensitivity of the main results to specification of these parameters. The base specification defines deprivation as being exposed to the top quartile of all tract-year exposure levels across the 168 cities, and sets the minimum number of deprivations at 2.

Graphs in the first two columns of Appendix Figure A1, recalculate Figure 2 changing the exposure threshold to the top tercile and top quintile, holding the minimum number of deprivations constant at 2. Gap magnitude declines slightly as the deprivation threshold increases, but the ordering of groups and trends over time do not change substantially.

Figure A2 recalculates Figure 5, depicting the impact of changes in the threshold quantile in multi-exposure gaps across cities. The size of the marker is proportional to the absolute value of parameter β_t^m. Consistent with Figure A1, increasing the threshold results in smaller and fewer significant gaps. Nevertheless, the overall pattern of a decrease in racial multi-exposure gaps across time persists, with the exception of a few cities primarily located in California's Central Valley.

Parameter k from Eq. (2) sets the minimum number of stressors for which an individual must be deprived to be considered extremely exposed. Here, we consider two alternatives (holding the threshold constant at the top quartile): $k = 0$, an individual is extremely exposed if deprived in *any* stressor; and $k = 3$, an individual is extremely only if deprived in *all* stressors. The graphs in the right two columns of Appendix Figure A1 show the effect of this parameter on trends in within-city gaps across time. Increasing the minimum number of stressors substantially reduces the magnitude of the gaps, but the patterns remain

similar. Appendix Figure A3 depicts the spatial distribution of changes in gaps across cities. Increasing the minimum number of stressors, reduces the number of cities with significant gaps in each period. Nonetheless, the general pattern of a reduction in cities with significant gaps over time persists across specifications, with all significant gaps being eliminated by 2020 if deprivations in all 3 stressors is required for being classified as extremely exposed.

5 Conclusion

A large literature has documented that minority and low-income populations experience disproportionate exposure to a variety of environmental stressors. The extent to which disparities exist for simultaneous exposure of the same individuals to multiple environmental stressors has been an unresolved question. Quantifying simultaneous exposure is important not only from the perspective of examining environmental disparities. It is also important for advancing our knowledge of potential health impacts of cross-stressor interaction effects.

This paper takes two first steps to deepen our understanding of simultaneous exposure. First, we show how recent methodological advances the analysis of multi-dimensional poverty literature can be adapted to rank distributions of extreme simultaneous exposure in a normatively significant way that accounts for frequency, breadth, and severity. Second, we apply these methods to examine trends in extreme simultaneous exposure to multi-exposure to $PM_{2.5}$, air toxics, and LST for race- and poverty-based demographic groups within and across 161 U.S. cities over two decades, from 2000–2020.

We find that in the case of single stressors, national median exposure to air toxics and $PM_{2.5}$ has fallen for all groups, while exposure to summer heat has increased. Consistent with the environmental justice literature, we find race- and poverty-based disparities in the distribution of individual environmental stressors. In the case of simultaneous extreme exposure, we find that such disparities exist, but have substantially fallen over time. Since above-poverty POC tend to have the same or worse outcomes than below-poverty non-Hispanic Whites, income does not appear to be a driving factor behind these results.

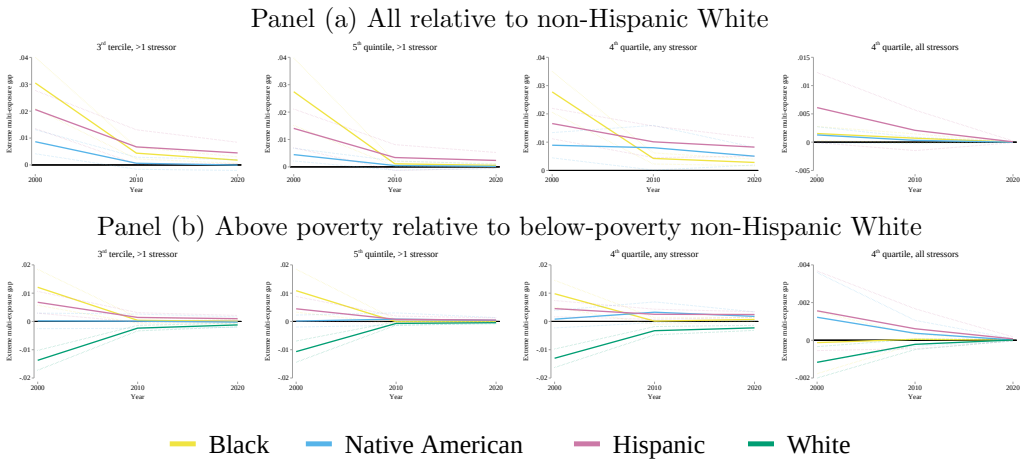
Disentangling the different components of the index, we find that there has been a large drop in the proportion of the extremely exposed in the general population for all groups, but particularly for below-poverty Black groups. Interestingly, we find that while severity exposure gaps for $PM_{2.5}$ and air toxics have decreased, exposure disparities in LST have widened, which partially offsets improvements in the other two stressors. These results highlight the importance of considering multiple, simultaneous sources of environmental stress when analyzing potential policy impacts, particularly in the case of disparities among the most exposed groups.

The methodological approach presented here has a range of potential applications in policy analysis. It could, for example, be used in conjunction with pollution dispersion modeling in the context of considering effects of regulatory options in EPA Regulatory Impact Analysis. Alternative regulatory approaches (e.g., emissions trading and technological pollution control requirements) generally have different implications for the spatial distribution of environmental stressors. This type of analysis could be presented to better understand which option is more desirable for the extremely exposed in general irrespective of demographic groupings. Further breaking down results by income or racial groups could also be useful for environmental justice analysis. Similarly, municipalities could use these methods to select urban heat mitigation strategies on the basis of which alternatives ameliorate impacts on those that suffer from extreme multi-exposure to other stressors. In addition to such prospective analyses these methods could be useful for retrospective analyses to better understand the roles of policy, geography, and climate on localized trends in extreme multi-exposure.

Empirical results presented here represent an initial exploration into extreme multi-exposure analysis, and as such have several limitations. We only consider three types of environmental stressors. Data permitting, it would be straightforward to include other sources of environmental stress (e.g., flood risk or water contamination) as well. Furthermore, research has found correlated disparities between environmental stressors and other social stressors (Bakkensen et al., 2024). Understanding how other socioeconomic stressors such as lack of access to health services or housing compound cumulative disparities is an important question for future research. Our empirical work uses data aggregated to the census tract level. Recent efforts have leveraged restricted-access census microdata to estimate disparities to different environmental stressors (Voorheis et al., 2024b) at the individual level. Although Voorheis et al. (2024a) find that assigning individuals their census tract's average concentrations, results in only a small attenuation of $PM_{2.5}$ exposure, this result may not apply to other environmental stressors or multi-exposure more generally. Finally, our analysis abstracts from migration, holding population fixed as of 2010. Access to microdata would allow exploration of the question of whether changes in multi-exposure lead to changes in census tract demographic composition along the lines suggested by Depro et al. (2015).

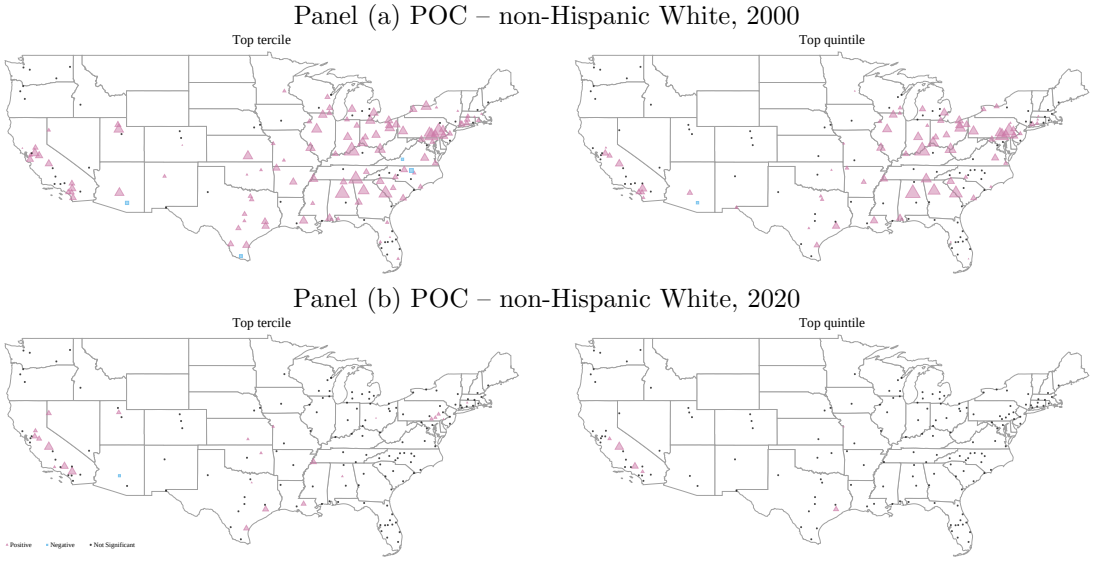
Appendix

Figure A1: Sensitivity of within-city gaps in extreme multi-exposure to parameter values



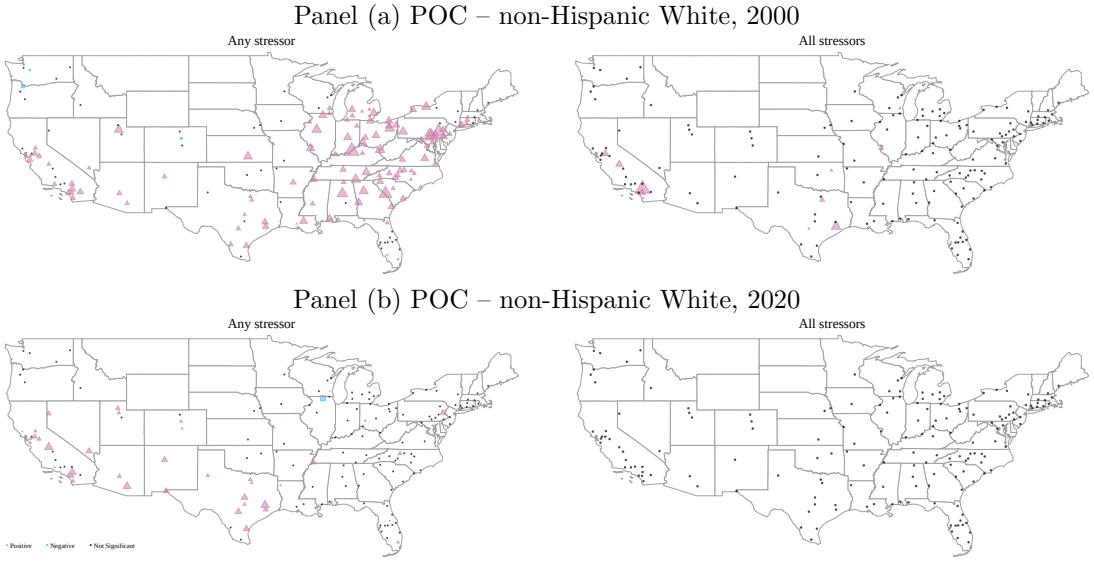
Notes: Panel (a) shows intra-city gaps in the multi-exposure index for Black, Native American, and Hispanic demographic groups relative to non-Hispanic White. Panel (b) shows gaps for above-poverty Black, Native American, Hispanic, and non-Hispanic White groups relative to below-poverty non-Hispanic White. Lines correspond to parameters β_t^m from Eq. (8). Regression specifications vary by quantile of exposure threshold for being deprived in a stressor, and the minimum number of deprived stressors to be considered extremely exposed. Regressions weighted by tract population for the relevant demographic groups. Standard errors clustered by city.

Figure A2: Differences across time in city-level demographic gaps in multiexposure index



Notes: "Top tercile" and "Top quintile" indicate the quantile defining the extremely exposed for each stressor. Significant ($p < 0.05$) within-city differences in extreme multi-exposure index between POC and non-Hispanic White. Significant ($p < 0.05$) positive values are depicted with triangles, significant negative values are depicted with squares, and statistically insignificant values are depicted with circles. Size of marker proportional to absolute value of significant difference. Standard errors clustered by census tract.

Figure A3: Differences across time in city-level demographic gaps in multiexposure index



Notes: "Any stressor" and "All stressors" indicate the minimum number of stressors to which an individual must be deprived to be classified as extremely exposed. Significant ($p < 0.05$) within-city differences in extreme multi-exposure index between POC and non-Hispanic White. Significant ($p < 0.05$) positive values are depicted with triangles, significant negative values are depicted with squares, and statistically insignificant values are depicted with circles. Size of marker proportional to absolute value of significant difference. Standard errors clustered by census tract.

References

Alkire, Sabina and James Foster. 2011. "Counting and Multidimensional Poverty Measurement." *Journal of Public Economics* 95:476–487.

Analitis, Antonis, Paola Michelozzi, Daniela D'Ippoliti, Francesca de'Donato, Bettina Menne, Franziska Matthies, Richard W. Atkinson, Carmen Iñiguez, Xavier Basagaña, Alexandra Schneider, Agnès Lefranc, Anna Paldy, Luigi Bisanti, and Klea Katsouyanni. 2014. "Effects of Heat Waves on Mortality: Effect Modification and Confounding by Air Pollutants." *Epidemiology* 25:15.

Ard, Kerry. 2015. "Trends in Exposure to Industrial Air Toxins for Different Racial and Socioeconomic Groups: A Spatial and Temporal Examination of Environmental Inequality in the U.S. from 1995 to 2004." *Social Science Research* 53:375–390.

Bakkensen, Laura A., Lala Ma, Lucija Muehlenbachs, and Lina Benitez. 2024. "Cumulative Impacts in Environmental Justice: Insights from Economics and Policy." *Regional Science and Urban Economics* 107:103993.

Banzhaf, Spencer, Lala Ma, and Christopher Timmins. 2019. "Environmental Justice: The Economics of Race, Place, and Pollution." *The Journal of Economic Perspectives: A Journal of the American Economic Association* 33:185–208.

Banzhaf, Spencer H. and Randall P. Walsh. 2008. "Do People Vote with Their Feet? An Empirical Test of Tiebout's Mechanism." *American Economic Review* 98:843–863.

Basu, Sayahnika, Jonathan D. Ketcham, and Nicolai V. Kuminoff. 2025. "Environmental Regulation, Residential Sorting, and Pollution Exposure among Senior Americans." *Journal of Environmental Economics and Management* 133:103211.

Besse, Hannah and David Rojas-Rueda. 2025. "Environmental Justice Mapping Tools in the United States: A Review of National and State Tools." *Science of The Total Environment* 962:178449.

Bolin, Bob, Eric Matranga, Edward J. Hackett, Edward K. Sadalla, K David Pijawka, Debbie Brewer, and Diane Sicotte. 2000. "Environmental Equity in a Sunbelt City: The Spatial Distribution of Toxic Hazards in Phoenix, Arizona." *Global Environmental Change Part B: Environmental Hazards* 2:11–24.

Borsky, Stefan, Eric Fesselmeyer, and Lennart Vogelsang. 2024. "Urban Heat and Within-City Residential Sorting." *Journal of Environmental Economics and Management* 127:103014.

Boucher, Jean Léon, Anthony M. Levenda, Caleb Carpenter, Jorge Morales-Guerrero, and Darshan M. A. Karwat. 2021. "Environmental Justice in Phoenix, Arizona: A Neighbourhood Deficit and Asset Score." *Local Environment* 26:692–718.

Boyce, James K., Klara Zwickl, and Michael Ash. 2016. "Measuring Environmental Inequality." *Ecological Economics* 124:114–123.

Cain, Lucas, Danae Hernandez-Cortes, Christopher Timmins, and Paige Weber. 2024. "Recent Findings and Methodologies in Economics Research in Environmental Justice." *Review of Environmental Economics and Policy* 18:116–142.

Chakraborty, Tirthankar, Andrew J. Newman, Yun Qian, Angel Hsu, and Glenn Sheriff. 2023. "Residential Segregation and Outdoor Urban Moist Heat Stress Disparities in the United States." *One Earth* 6.

Chakraborty, T., Z. S. Venter, Y. Qian, and X. Lee. 2022. "Lower Urban Humidity Moderates Outdoor Heat Stress." *AGU Advances* 3:e2022AV000729.

Chen, Kai, Kathrin Wolf, Susanne Breitner, Antonio Gasparrini, Massimo Stafoggia, Evangelia Samoli, Zorana Jovanovic Andersen, Getahun Bero-Bedada, Tom Bellander, Frauke Hennig, Bénédicte Jacquemin, Juha Pekkanen, Regina Hampel, Josef Cyrys, Annette Peters, and Alexandra Schneider. 2018. "Two-Way Effect Modifications of Air Pollution and Air Temperature on Total Natural and Cardiovascular Mortality in Eight European Urban Areas." *Environment International* 116:186–196.

Colmer, Jonathan, Ian Hardman, Jay Shimshack, and John Voorheis. 2020. "Disparities in PM2.5 Air Pollution in the United States." *Science* 369:575–578.

Colmer, Jonathan, Suvy Qin, John Voorheis, and Reed Walker. 2024. "The Changing Nature of Pollution, Income, and Environmental Inequality in the United States." *AEA Papers and Proceedings* 114:41–46.

Crawford, Christopher J., David P. Roy, Saeed Arab, Christopher Barnes, Eric Vermote, Glynn Hulley, Aaron Gerace, Mike Choate, Christopher Engebretson, Esad Micijevic, Gail Schmidt, Cody Anderson, Martha Anderson, Michelle Bouchard, Bruce Cook, Ray Dittmeier, Danny Howard, Calli Jenkerson, Minsu Kim, Tania Kleyians, Thomas

Maiersperger, Chase Mueller, Christopher Neigh, Linda Owen, Benjamin Page, Nima Pahlevan, Rajagopalan Rengarajan, Jean-Claude Roger, Kristi Sayler, Pat Scaramuzza, Sergii Skakun, Lin Yan, Hankui K. Zhang, Zhe Zhu, and Steve Zahn. 2023. "The 50-Year Landsat Collection 2 Archive." *Science of Remote Sensing* 8:100103.

Currie, Janet, John Voorheis, and Reed Walker. 2023. "What Caused Racial Disparities in Particulate Exposure to Fall? New Evidence from the Clean Air Act and Satellite-Based Measures of Air Quality." *American Economic Review* 113:71–97.

Cushing, Lara, John Faust, Laura Meehan August, Rose Cendak, Walker Wieland, and George Alexeeff. 2015. "Racial/Ethnic Disparities in Cumulative Environmental Health Impacts in California: Evidence From a Statewide Environmental Justice Screening Tool (CalEnviroScreen 1.1)." *American Journal of Public Health* 105:2341–2348.

Depro, Brooks, Christopher Timmins, and Maggie O'Neil. 2015. "White Flight and Coming to the Nuisance: Can Residential Mobility Explain Environmental Injustice?" *Journal of the Association of Environmental and Resource Economists* 2:439–468.

Escher, Beate I., Heather M. Stapleton, and Emma L. Schymanski. 2020. "Tracking Complex Mixtures of Chemicals in Our Changing Environment." *Science* 367:388–392.

Faust, John, Laura August, Andrew Slocombe, Shankar Prasad, Walker Wieland, Vincent Cogliano, and Carol Monahan Cummings. 2021. "California's Environmental Justice Mapping Tool: Lessons and Insights from CalEnviroScreen." *Environmental Law Reporter* 51:10684.

Gamper-Rabindran, Shanti. 2006. "Did the EPA's Voluntary Industrial Toxics Program Reduce Emissions? A GIS Analysis of Distributional Impacts and by-Media Analysis of Substitution." *Journal of Environmental Economics and Management* 52:391–410.

Hernandez-Cortes, Danae and Kyle C. Meng. 2023. "Do Health Disparities Narrow with Pollution Disparities? Trends from California." *AEA Papers and Proceedings* 113:372–376.

Hsu, Angel, Glenn Sheriff, Tirthankar Chakraborty, and Diego Manya. 2021. "Disproportionate Exposure to Urban Heat Island Intensity across Major US Cities." *Nature Communications* 12:2721.

Joseph, Lesley. 2025. "Towards a More Comprehensive Environmental Justice Index: A Critical Review of Existing Indicators and Indices." *Journal of Environmental Planning and Management* pp. 1–34.

Jowers, Kay, Yu Ma, and Christopher Timmins. 2025. "The Equity Implications of Exposure to Industrial Livestock Operations."

Kaufman, Joel D., Sara D. Adar, Ryan W. Allen, R. Graham Barr, Matthew J. Budoff, Gregory L. Burke, Adrian M. Casillas, Martin A. Cohen, Cynthia L. Curl, Martha L. Daviglus, Ana V. Diez Roux, David R. Jacobs, Jr., Richard A. Kronmal, Timothy V. Larson, Sally Lee-Jane Liu, Thomas Lumley, Ana Navas-Acien, Daniel H. O'Leary, Jerome I. Rotter, Paul D. Sampson, Lianne Sheppard, David S. Siscovick, James H. Stein, Adam A. Szpiro, and Russell P. Tracy. 2012. "Prospective Study of Particulate Air Pollution Exposures, Subclinical Atherosclerosis, and Clinical Cardiovascular Disease: The Multi-Ethnic Study of Atherosclerosis and Air Pollution (MESA Air)." *American Journal of Epidemiology* 176:825–837.

Khanna, Neha. 2000. "Measuring Environmental Quality: An Index of Pollution." *Ecological Economics* 35:191–202.

Khomsi, Kenza, Youssef Chelhaoui, Soukaina Alilou, Rania Souri, Houda Najmi, and Zineb Souhaili. 2022. "Concurrent Heat Waves and Extreme Ozone (O3) Episodes: Combined Atmospheric Patterns and Impact on Human Health." *International Journal of Environmental Research and Public Health* 19:2770.

Krieg, Eric J. and Daniel R. Faber. 2004. "Not so Black and White: Environmental Justice and Cumulative Impact Assessments." *Environmental Impact Assessment Review* 24:667–694.

Lara Ibarra, Gabriel, Minh Cong Nguyen, Daylan Alberto Salmeron Gomez, and Cameron Nadim Haddad. 2025. "October 2025 Update to the Multidimensional Poverty Measure: What's New." Global Poverty Monitoring Technical Note 49, World Bank Group, Washington, DC.

Lee, Charles. 2020. "A Game Changer in the Making? Lessons from States Advancing Environmental Justice through Mapping and Cumulative Impact Strategies." *Environmental Law Reporter* 50:10203–10215.

Lefler, Jacob S., Joshua D. Higbee, Richard T. Burnett, Majid Ezzati, Nathan C. Coleman, Dalton D. Mann, Julian D. Marshall, Matthew Bechle, Yuzhou Wang, and Allen L. Robinson. 2019. "Air Pollution and Mortality in a Large, Representative US Cohort: Multiple-Pollutant Analyses, and Spatial and Temporal Decompositions." *Environmental Health* 18:1–11.

Liu, Jiawen, Lara P. Clark, Matthew J. Bechle, Anjum Hajat, Sun-Young Kim, Allen L. Robinson, Lianne Sheppard, Adam A. Szpiro, and Julian D. Marshall. 2021. "Disparities in Air Pollution Exposure in the United States by Race/Ethnicity and Income, 1990–2010." *Environmental Health Perspectives* 129:127005.

Madrigano, Jaime, Darby Jack, G. Brooke Anderson, Michelle L. Bell, and Patrick L. Kinney. 2015. "Temperature, Ozone, and Mortality in Urban and Non-Urban Counties in the Northeastern United States." *Environmental Health* 14:3.

Morello-Frosch, Rachel, Manuel Pastor, and James Sadd. 2001. "Environmental Justice and Southern California's "Riskscape": The Distribution of Air Toxics Exposures and Health Risks Among Diverse Communities." *Urban Affairs Review* 36:551–578.

Nunez, Yanelli, Jaime Benavides, Jenni A. Shearston, Elena M. Krieger, Misbath Daouda, Lucas R. F. Henneman, Erin E. McDuffie, Jeff Goldsmith, Joan A. Casey, and Marianthi-Anna Kioumourtzoglou. 2024. "An Environmental Justice Analysis of Air Pollution Emissions in the United States from 1970 to 2010." *Nature Communications* 15:268.

OPHI and UNDP. 2025. "Global Multidimensional Poverty Index 2025 – Overlapping Hardships: Poverty and Climate Hazards." Technical report, Oxford Poverty and Human Development Initiative (OPHI) and United Nations Development Programme (UNDP).

Pearce, Jamie R, Elizabeth A Richardson, Richard J Mitchell, and Niamh K Shortt. 2010. "Environmental Justice and Health: The Implications of the Socio-Spatial Distribution of Multiple Environmental Deprivation for Health Inequalities in the United Kingdom." *Transactions of the Institute of British Geographers* 35:522–539.

Pollack, Adam B., Sara Santamaria-Aguilar, Pravin Maduwantha, Casey Helgeson, Thomas Wahl, and Klaus Keller. 2025. "Funding Rules That Promote Equity in Climate Adaptation Outcomes." *Proceedings of the National Academy of Sciences* 122:e2418711121.

Pope III, C. Arden, Richard T. Burnett, Michael J. Thun, Eugenia E. Calle, Daniel Krewski, Kazuhiko Ito, and George D. Thurston. 2002. "Lung Cancer, Cardiopulmonary Mortality, and Long-term Exposure to Fine Particulate Air Pollution." *Journal of the American Medical Association* 287:1132–1141.

Rahman, Md Mostafijur, Rob McConnell, Hannah Schlaerth, Joseph Ko, Sam Silva, Frederick W. Lurmann, Lawrence Palinkas, Jill Johnston, Michael Hurlburt, Hao Yin, George Ban-Weiss, and Erika Garcia. 2022. "The Effects of Coexposure to Extremes of Heat and

Particulate Air Pollution on Mortality in California: Implications for Climate Change." *American Journal of Respiratory and Critical Care Medicine* 206:1117–1127.

Rai, Masna, Massimo Stafoggia, Francesca de'Donato, Matteo Scortichini, Sofia Zafeiratou, Liliana Vazquez Fernandez, Siqi Zhang, Klea Katsouyanni, Evangelia Samoli, Shilpa Rao, Eric Lavigne, Yuming Guo, Haidong Kan, Samuel Osorio, Jan Kyselý, Aleš Urban, Hans Orru, Marek Maasikmets, Jouni J. K. Jaakkola, Niilo Ryti, Mathilde Pascal, Masahiro Hashizume, Chris Fook Sheng Ng, Barrak Alahmad, Magali Hurtado Diaz, César De la Cruz Valencia, Baltazar Nunes, Joana Madureira, Noah Scovronick, Rebecca M. Garland, Ho Kim, Whanhee Lee, Aurelio Tobias, Carmen Íñiguez, Bertil Forsberg, Christofer Åström, Ana Maria Vicedo-Cabrera, Martina S. Ragettli, Yue-Liang Leon Guo, Shih-Chun Pan, Shanshan Li, Antonio Gasparrini, Francesco Sera, Pierre Masselot, Joel Schwartz, Antonella Zanobetti, Michelle L. Bell, Alexandra Schneider, and Susanne Breitner. 2023. "Heat-Related Cardiorespiratory Mortality: Effect Modification by Air Pollution across 482 Cities from 24 Countries." *Environment International* 174:107825.

Sadd, James L., Manuel Pastor, Rachel Morello-Frosch, Justin Scoggins, and Bill Jesdale. 2011. "Playing It Safe: Assessing Cumulative Impact and Social Vulnerability through an Environmental Justice Screening Method in the South Coast Air Basin, California." *International Journal of Environmental Research and Public Health* 8:1441–1459.

Sager, Lutz. 2025. "Global Air Quality Inequality over 2000–2020." *Journal of Environmental Economics and Management* 130:103112.

Scaramuzza, Pasquale and Julia Barsi. 2005. "Landsat 7 Scan Line Corrector-off Gap-Filled Product Development." In *Proceeding of Pecora*, volume 16, pp. 23–27.

Scortichini, Matteo, Manuela De Sario, Francesca K. De'Donato, Marina Davoli, Paola Michelozzi, and Massimo Stafoggia. 2018. "Short-Term Effects of Heat on Mortality and Effect Modification by Air Pollution in 25 Italian Cities." *International Journal of Environmental Research and Public Health* 15:1771.

Shen, Siyuan, Chi Li, Aaron van Donkelaar, Nathan Jacobs, Chenguang Wang, and Randall V. Martin. 2024. "Enhancing Global Estimation of Fine Particulate Matter Concentrations by Including Geophysical a Priori Information in Deep Learning." *ACS ES&T Air* 1:332–345.

Sheriff, Glenn and Kelly Maguire. 2020. "Health Risk, Inequality Indexes, and Environmental Justice." *Risk Analysis* 40:2661–2674.

Sicotte, Diane. 2010. "Some More Polluted than Others: Unequal Cumulative Industrial Hazard Burdens in the Philadelphia MSA, USA." *Local Environment* 15:761–774.

Tessum, Christopher W., David A. Paolella, Sarah E. Chambliss, Joshua S. Apte, Jason D. Hill, and Julian D. Marshall. 2021. "PM2.5 Polluters Disproportionately and Systemically Affect People of Color in the United States." *Science Advances* 7:eabf4491.

UNDP. 2025. "Human Development Report 2025: A Matter of Choice: People and Possibilities in the Age of AI." Technical report, United Nations Development Programme.

US EPA, OCSPP. 2019. "Risk-Screening Environmental Indicators (RSEI) Methodology Version 2.3.8." Data and Tools.

van Donkelaar, Aaron, Melanie S. Hammer, Liam Bindle, Michael Brauer, Jeffery R. Brook, Michael J. Garay, N. Christina Hsu, Olga V. Kalashnikova, Ralph A. Kahn, Colin Lee, Robert C. Levy, Alexei Lyapustin, Andrew M. Sayer, and Randall V. Martin. 2021. "Monthly Global Estimates of Fine Particulate Matter and Their Uncertainty." *Environmental Science & Technology* 55:15287–15300.

Venmans, Frank and Ben Groom. 2021. "Social Discounting, Inequality Aversion, and the Environment." *Journal of Environmental Economics and Management* 109:102479.

Voorheis, John, Jonathan Colmer, Kendall Houghton, Eva Lyubich, Mary Munro, Cameron Scalera, and Jennifer Withrow. 2024a. "The Census Environmental Impacts Frame."

Voorheis, John, Jonathan Colmer, Kendall Houghton, Eva Lyubich, Mary Munro, Cameron Scalera, and Jennifer Withrow. 2024b. "The Privacy-Protected Gridded Environmental Impacts Frame." US Census Bureau Working Papers 24-74, Center for Economic Studies.

Wang, Yuzhou, Joshua S. Apte, Jason D. Hill, Cesunica E. Ivey, Dana Johnson, Esther Min, Rachel Morello-Frosch, Regan Patterson, Allen L. Robinson, Christopher W. Tessum, and Julian D. Marshall. 2023. "Air Quality Policy Should Quantify Effects on Disparities." *Science* 381:272–274.

Wheeler, Benedict W. and Yoav Ben-Shlomo. 2005. "Environmental Equity, Air Quality, Socioeconomic Status, and Respiratory Health: A Linkage Analysis of Routine Data from the Health Survey for England." *Journal of Epidemiology & Community Health* 59:948–954.

Wulder, Michael A., David P. Roy, Volker C. Radeloff, Thomas R. Loveland, Martha C. Anderson, David M. Johnson, Sean Healey, Zhe Zhu, Theodore A. Scambos, Nima Pahlevan,

Matthew Hansen, Noel Gorelick, Christopher J. Crawford, Jeffrey G. Masek, Txomin Hermosilla, Joanne C. White, Alan S. Belward, Crystal Schaaf, Curtis E. Woodcock, Justin L. Huntington, Leo Lymburner, Patrick Hostert, Feng Gao, Alexei Lyapustin, Jean-Francois Pekel, Peter Strobl, and Bruce D. Cook. 2022. "Fifty Years of Landsat Science and Impacts." *Remote Sensing of Environment* 280:113195.

York, Abigail, Joseph Tuccillo, Christopher Boone, Bob Bolin, Lauren Gentile, Briar Schoon, and Kevin Kane. 2014. "Zoning and Land Use: A Tale of Incompatibility and Environmental Injustice in Early Phoenix." *Journal of Urban Affairs* 36:833–853.

Zippel, Claire, Matt Saenz, Raheem Chaudhry, and Vincent Palacios. 2023. "GETCENSUS: Stata Module to Load American Community Survey Data from the U.S. Census Bureau API into Stata." Boston College Department of Economics.

Zwickl, Klara, Michael Ash, and James K. Boyce. 2014. "Regional Variation in Environmental Inequality: Industrial Air Toxics Exposure in U.S. Cities." *Ecological Economics* 107:494–509.